

THE ORIGIN OF HEMATITE IN HIGH-GRADE IRON ORES BASED ON INFRARED MICROSCOPY AND FLUID INCLUSION STUDIES: THE EXAMPLE OF THE CONCEIÇÃO MINE, QUADRILÁTERO FERRÍFERO, BRAZIL

CARLOS ALBERTO ROSIÈRE†

Instituto de Geociências, Universidade Federal de Minas Gerais, 31270-901 Belo Horizonte MG, Brazil

AND FRANCISCO JAVIER RIOS

*Fluid Inclusion and Metallogenic Laboratory (EC1), Centro de Desenvolvimento da Tecnologia Nuclear (CDTN-CNEN),
Cx. Postal 941, 30123-970 Belo Horizonte MG, Brazil*

Abstract

Petrographic and textural analysis combined with fluid inclusion studies by infrared microscopy of high-grade (>65% Fe) hematite ore samples from the Conceição deposit, in the northeastern part of the Quadrilátero Ferrífero, Brazil, indicate a complex process of oxidation and mineralization during two orogenic events, each developed under different conditions and involving distinct fluids. The earliest mineralization formed massive magnetite-rich orebodies under relatively reducing conditions in the early stages of the Transamazonian orogeny. Magnetite was oxidized (martitized) with the development of porous hematite crystals (hematite I). Possibly during this stage, new hematite crystals were also formed from low-temperature, low- to medium-salinity fluids, as indicated by two-phase fluid inclusions. The origin of these fluids is still uncertain but tentatively interpreted as being modified surface water. The fluids were transported along normal faults and fractures during post-tectonic collapse following the Transamazonian orogeny (2.1–2.0 Ga) and creation of the dome-and-keel structural pattern of the Quadrilátero Ferrífero. These solutions were also likely responsible for the initial oxidation of the iron formations and the development of hematite I. Subsequent uplifted hot basement rocks or post-tectonic plutons were probable heat sources for the regional metamorphism and development of a granoblastic fabric of hematite II grains in the iron formations and high-grade orebodies. However, the ore was only partially recrystallized, as several relics of the early magnetite, martite, and hematite are still preserved in the granular hematite II crystals. During the Brasiliano-Pan-African orogeny (0.8–0.6 Ga), high-salinity fluids, with temperatures varying from ~120° to a maximum of approximately 350°C, penetrated the iron formations along shear zones, crystallizing initially tabular and thereafter platy hematite crystals (hematite III and specularite) forming schistose orebodies. Quartz veins that cut across the ore and envelop specularite plates and ore fragments formed from late-stage, high-temperature, and low-salinity fluids containing CO₂. These later fluids did not alter the ore.

Each of these stages of mineralization produced orebodies with distinct features. Recurrent hydrothermal mineralization is thought to have been responsible for the development of giant, high-grade iron ore deposits in structurally favorable sites. Fold hinges with enhanced permeability and deep faults able to conduct the fluids to the surface, repeatedly over time, should be important targets for exploration of new resources.

Introduction

The economically important, giant iron ore deposits of the Quadrilátero Ferrífero district, Minas Gerais, southeastern Brazil, are host to metamorphosed iron formations, referred to as itabirites, of the Paleoproterozoic Itabira Group. Concordant and discordant, hard, massive orebodies consisting of magnetite-martite and hematite occur together with structurally controlled, schistose, high-grade bodies and with friable weathered ores. The range of different types of iron orebodies has led to considerable debate about their origins. Two end-member genetic models have been proposed: supergene versus hydrothermal enrichment of a banded iron formation protore. In the case of the Hamersley and Animikie basins, several authors have suggested that hypogene enrichment by metasomatic replacement was responsible for mineralization (Gruner, 1924, 1930, 1937; Morey, 1999; Powell et al., 1999). Guild (1953, 1957) and Dorr (1965, 1969) postulated a similar origin for the Brazilian ores from the Quadrilátero Ferrífero. Taylor et al. (2001) provided an alternative interpretation for the role of hydrothermal fluids, whereby residual

enrichment through SiO₂ leaching was the principal mechanism for upgrading the ore. The importance of deformation in the concentration of hematite was also emphasized by Taylor et al. (2001) who established that the deposits from the Hamersley province are associated with medium-scale, normal faults that acted as channelways for the mineralizing fluids. Morey (1999) and Powell et al. (1999) proposed a compressional setting for the mineralization in the Hamersley province and Mesabi Range with synorogenic fluids driven by a regional tectonic gradient. Guild (1953, 1957) and Guba (1982) considered that the high-grade orebodies of Minas Gerais formed by iron remobilization, controlled by shear zones and hinges of meter-scale folds. Leith (1903), Van Hise and Leith (1911), Leith et al. (1935), Dorr (1964), Morris (1983), and Taylor et al. (2001) all considered that supergene enrichment by descending meteoric solutions was an important mineralizing process for the high-grade bodies in each of these districts.

It is likely that these different processes represent steps in a complex succession leading to the present shape and appearance of the different orebodies, as proposed by Taylor et al. (2001). In a first attempt to establish the nature and composition of the fluids involved and the conditions that

† Corresponding author: e-mail, crosiere@dedalus.lcc.ufmg.br

prevailed during oxidation and mineralization of the banded iron formation protore in the Quadrilátero Ferrífero, textural analysis together with microthermometric studies of different generations of hematite and specularite were conducted on samples from the Conceição deposit, located in the northeasternmost part of the district. Previous detailed petrographic and microstructural analyses, leading to the identification of several distinct hematite and specularite generations, are used as a basis for this study (Rosière, 1981; Rosière and Chemale, 1991; Rosière et al., 2001).

The Quadrilátero Ferrífero District

The Quadrilátero Ferrífero is located at the southern border of the São Francisco craton, a geotectonic unit of Brasiliano age (0.8–0.6 Ga), surrounded by the converging Araçuaí, Brasília, Rio Preto, Riacho do Pontal, and Sergipano orogenic belts (Dorr, 1969; Almeida, 1977; Schobbenhaus et al., 1984). The structure of the Quadrilátero Ferrífero (Fig. 1a) is defined by a roughly rectangular arrangement of synclines, with Paleoproterozoic metasedimentary rocks of the Minas Supergroup separated by antiformal structures dominated by Archean greenstones of the Rio das Velhas Supergroup and domes of Archean and Proterozoic crystalline rocks (Machado and Carneiro, 1992; Machado et al., 1992; Noce, 1995). The youngest ages for basement rocks are 2612 ± 5 Ma (Noce, 1995) and 2593^{+10}_{-19} Ma (Romano, 1989), for the Salto do Paraopeba and Florestal granites, respectively. The Minas Supergroup comprises, from bottom to top, the Caraça, Itabira, Piracicaba, and Sabará Groups (Dorr, 1969). The thickest sequence of iron formations together with enclosing high-grade iron orebodies belong to the Itabira Group, comprising itabirite, dolomite, and subordinate metapelite units. Carbonate rocks of the upper Itabira Group, which contain algal remnants, have been dated by Babinski et al. (1995) at 2419 ± 19 Ma (Pb-Pb isochron data). Carbonate rocks of the Piracicaba Group, in contrast, yielded Pb-Pb ages of 2050 ± 230 Ma, which are interpreted to be metamorphic ages (Babinski et al., 1995). The Sabará Group comprises a 3.0- to 3.5-km-thick sequence of metavolcanoclastic rocks, turbidites and conglomerates, separated by an unconformity from the underlying Piracicaba Group. Based on U-Pb dating of detrital zircons, Machado et al. (1989, 1992) postulated a depositional age of 2125 Ma.

The regional structure is the result of the superposition of two main deformation events (Chemale, Jr. et al., 1994). The first produced the nucleation of regional synclines in the supracrustal sequence, uplifting of the gneissic domes during the Transamazonian orogenesis (2.1–2.0 Ga), and the regional metamorphism. The second was related to a west-verging thrust belt of Brasiliano/Pan-African age (0.8–0.6 Ga; tectonic transport arrows, Fig. 1a). The latter event, which was more dramatic in the eastern half of the Quadrilátero Ferrífero, deformed the earlier structures and was responsible for the deformation gradient present in the area and possibly for the metamorphic gradient determined by Pires (1995). Two main structural domains (Rosière et al., 2001) can be delimited regionally (Fig. 1). The eastern high-strain domain includes regional thrust systems and shear zones that may be several hundred meter wide, whereas the western low-strain domain displays well-preserved megasynclines that are discontinuously

cut by discrete shear zones and faults. The iron formation of the Itabira Group delineates the main structures of the entire Quadrilátero Ferrífero as a regional marker (Fig. 1b), and high-grade iron deposits occur along the limbs of the megasynclines as well as in shear zones in the eastern high-strain domain.

The main regional thermal metamorphic event in the Quadrilátero Ferrífero is related to the late extensional phase of the Transamazonian event and predates the pervasive foliation developed during the Brasiliano orogenesis and the formation of specularite (Chemale, Jr. et al., 1994; Alkmim and Marshak, 1998; Rosière et al., 2001). Regional metamorphic zoning is defined by the presence of chlorite, biotite, and staurolite (Herz, 1978), with metamorphic grade increasing eastward, and the zoning roughly follows the deformation gradient. Pires (1995) redefined the zones of grunerite (GZ), cummingtonite (CZ), actinolite (AZ), and tremolite-antophyllite (TAZ) (Fig. 1b) based on the metamorphic mineralogy of the iron formations of the Itabira Group. Thermal aureoles surrounding the domes, however, interfere with this zoning and produce a local higher grade metamorphic overprint (Herz, 1978; Marshak et al., 1992).

Itabirites and Iron Ores of the Itabira Group

The Itabira Group is a sequence of predominantly chemical, sedimentary rocks deposited in a platformal marine environment and is composed of two formations (Dorr, 1969): the Cauê Formation, which comprises a thick sequence (ca. 250–300 m) of iron formations (itabirites and hematite bodies) intercalated with hematitic phyllites, dolomitic phyllites and marbles; and the Gandarela Formation, which conformably overlies the Cauê Formation and is composed of carbonate rocks (calcitic and dolomitic marbles) with subordinate phyllites and banded iron formation.

The name itabirite is used to describe metamorphosed, oxidized, and heterogeneously deformed banded iron formations (Dorr, 1969). There are several distinct mineralogical and textural types due to variation in the original composition of the sediments, intensity of deformation, and degree of metamorphism and hydrothermal alteration.

Hard, high-grade iron ore occurs both as massive and as schistose bodies within the itabirite. The shape of the massive orebodies is totally or partially controlled by the bedding of the banded iron formation protore, and the granoblastic fabric commonly mimics the original structure. Irregular pockets of high-grade iron ore with a brecciated fabric may also occur but are not as common. Schistose orebodies occupy shear zones that crosscut the banded iron formation.

Mineralogy of the Iron Oxides in the Quadrilátero Ferrífero

Microcrystalline hematite (primary hematite) and other minerals, typical of very low grade metamorphic banded iron formations such as in the Hamersley Range (Trendall and Blockley, 1970) or in the Transvaal/Griqualand areas (Beukes, 1984) have not been observed in the itabirites of the Quadrilátero Ferrífero. Magnetite both in the itabirite and high-grade orebodies is typically kenomagnetite (Kullerud et al., 1969; Morris, 1980; Rosière, 1981), an Fe²⁺-deficient variety, which is found ubiquitously in low-strain portions of the

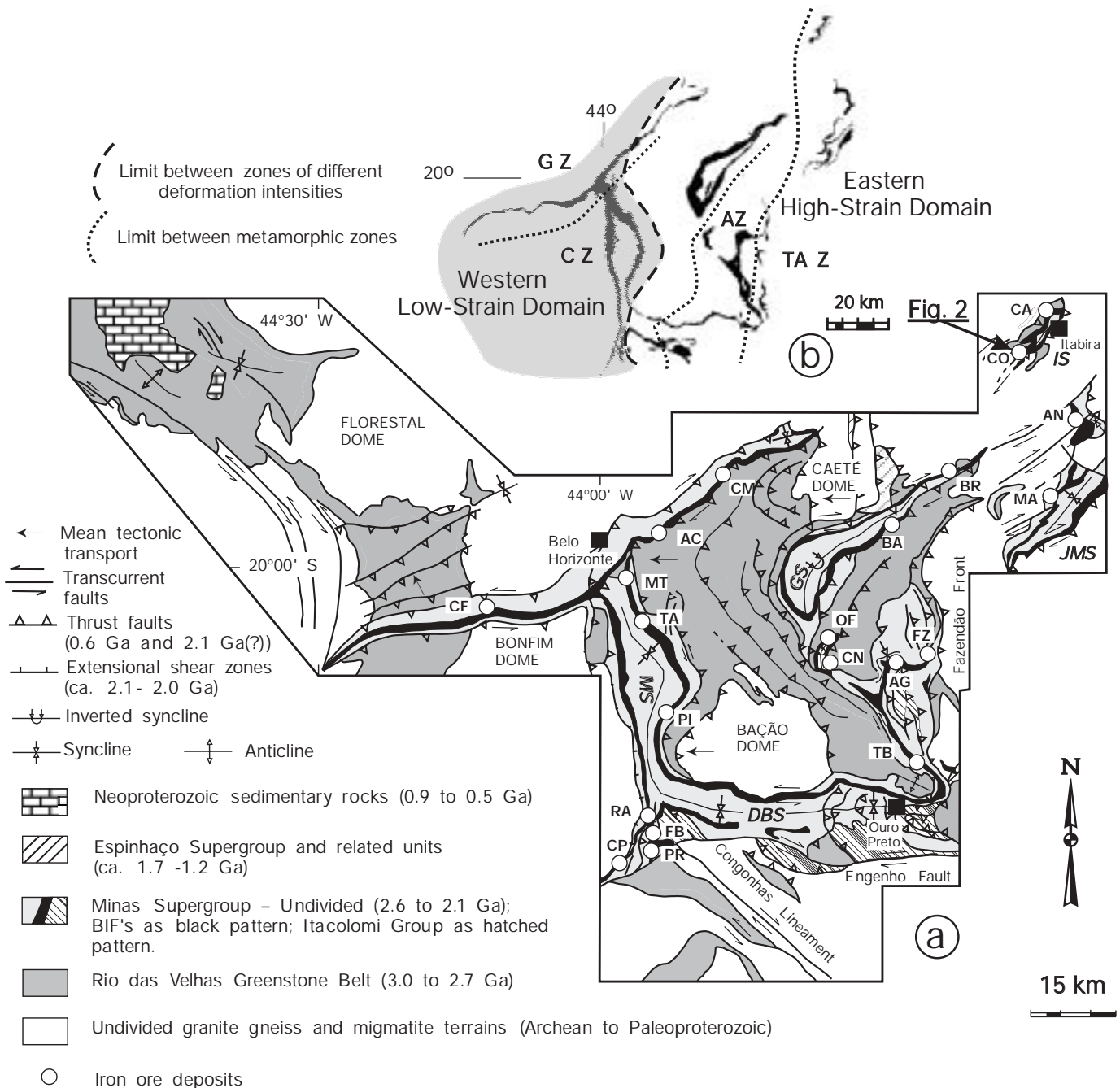


FIG. 1. (a). Geologic map of the Quadrilátero Ferrífero (modified after Dorr, 1969; Baars and Rosière, 1997). Major tectonic structures: DBS = Dom Bosco syncline, GS = Gandarela syncline, IS = Itabira synclinorium, JMS = João Monlevade synclinorium, MS = Moeda syncline. Main iron ore deposits: AC = Águas Claras, AG = Alegria, AN = Andrade, BA = Baú, BR = Brucutu, CA = Cauê, CF = Córrego do Feijão, CM = Córrego do Meio, CN = Capanema, CO = Conceição, CP = Casa de Pedra, FB = Fábrica, FZ = Fazendão, MA = Morro Agudo, MT = Mutuca, OF = Ouro Fino, PI = Pico do Itabirito, PR = Pires, RA = Retiro das Almas, TA = Tamanduá, TB = Timbopeba. Inset shows the location of the Conceição deposit detailed in Figure 2. (b). Location of metamorphic and structural domains in the Quadrilátero Ferrífero. Shaded area depicts the low strain domain. Metamorphic zones after Pires (1995): AZ = Actinolite zone, CZ = Cummingtonite zone, GZ = Grunerite zone, TAZ = Tremolite-Antophyllite zone. Banded iron formation of the Itabira Group is shown in black.

ore, mainly in the western domain of the Quadrilátero Ferrífero, and is interpreted to be the oldest iron oxide of the assemblage. Magnetite normally occurs as relics in martite (hematite pseudomorphous after magnetite) and in hematite aggregates or even by itself in some bodies. The

high abundance of magnetite relics indicates that it was the main iron oxide of iron formation and high-grade ores in the Itabira Group, prior to the oxidation that affected the entire Cauê Formation and resulted in rocks containing predominantly hematite (Rosière, 1981).

In the western low-strain domain of the Quadrilátero Ferrífero, hematite occurs mainly as subhedral to euhedral granular crystals (0.01–0.2 mm) and, together with anhedral grains, has an overall granoblastic fabric. This fabric is considered to represent post-tectonic partial recrystallization (Rosière 1981; Rosière et al., 2001).

In shear zones, which are more pervasive in the eastern high-strain domain, hematite commonly occurs as euhedral, tabular-shaped or very elongated specularite platelets, which commonly overgrow relics of granoblastic aggregates (similar to those found in the western domain) or occur in strain shadow microdomains. Specularite plates are syntectonic, have a preferred orientation, and define a schistosity of variable intensity and penetration with the development of a wide variety of deformational and metamorphic fabrics (Rosière et al., 2001).

The Conceição Iron Ore Deposit

The Conceição deposit is the southernmost of the Itabira Complex in the northeastern part of the Quadrilátero Ferrífero

(Fig. 1a). The mine is operated as an open pit by the Companhia Vale do Rio Doce (CVRD) and is located in the re-folded hinge zone of the Conceição syncline, one of the folds that compose the Itabira synclinorium, which is the main regional structure in the area (Fig. 1a). The rocks in the northeastern extremity of the Quadrilátero Ferrífero experienced high strain during the Brasiliano orogeny (Chemale, Jr. et al., 1994) with the development of shear zones, tight folds, and partial transposition of the primary banding of the itabirite. In the Conceição syncline two main schistosities developed. These are S_1 , which developed during the first-generation folding F_1 , and S_2 , which is axial planar to the second-generation folds F_2 (Chemale et al., 1987, Rosière et al., 1997). The latter schistosity is related to northeast-trending transpression, during which thrust sheets interacted with the 1.670 ± 32 Ma Borrachudos granite intrusive body (Chemale et al., 1994; Chemale et al., 1997). In the Conceição deposit, F_1 and F_2 folds are coaxial, plunging 40 to N 60 E and the macroscopic structure represents a classical type 3 interference pattern of Ramsay (1962; Fig. 2).

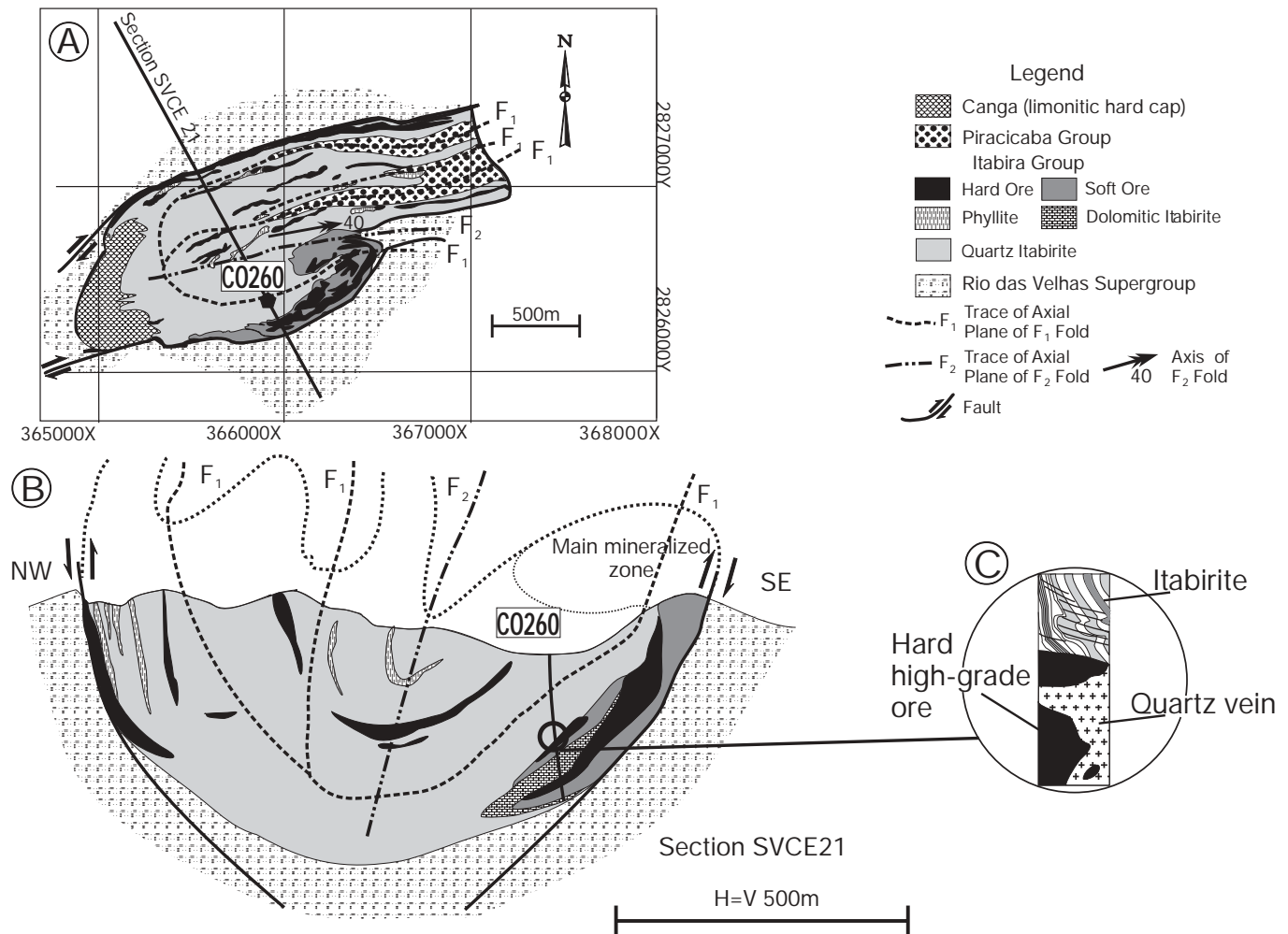


FIG. 2. (a). Simplified geologic map of the Conceição iron ore deposit, showing the location of CO260 diamond drill hole, based on data furnished by the Companhia Vale do Rio Doce as well our own observations and mapping. (b). Schematic representation of cross section SCVCE21, showing the location of analyzed samples in diamond drill hole CO260. Map and section are referenced to mine internal coordinate system. (c). Schematic drawing of the analyzed core sample.

Metamorphic mineral assemblages in the rocks of the Minas Supergroup surrounding the Conceição deposit indicate intermediate-grade metamorphic conditions between upper greenschist and lower amphibolite facies, with temperatures of about 450°C (Dorr and Barbosa, 1963; Schorscher, 1975; Herz, 1978; Chemale, 1987; Pires, 1995). Schorscher (1975) placed the staurolite isograd only 4 km northeast of the Itabira district, whereas Pires (1995) located it just west of the Conceição deposit (Fig. 1b). Oxygen isotope studies of the iron ores and itabirites in the area (e.g., Hoefs et al., 1982; Müller et al., 1986) indicate even higher metamorphic temperatures with sharp local variations (408°–660°C).

Analyzed Samples and Petrographic Characteristics under Reflected Light

In order to study the origin of the fluids related to the oxidation and enrichment processes in itabirites and the high-grade orebodies, infrared microscopic analysis and fluid inclusion studies were carried out on doubly polished thin sections. These were prepared from samples of hard ore and quartz veins collected from the diamond drill core CO260 located at the southern part of the Conceição deposit (hole CO260, Fig. 2). The sampled section extends from the lower contact zone between the moderately deformed high-grade massive orebody and itabirite protore and is crosscut by discrete microshear zones.

The samples were grouped into three types: samples of massive ore, samples from a shear zone cutting the massive ore, and samples from a quartz vein.

The massive high-grade ore consists of hematite grains with variable characteristics (Table 1) and martite aggregates with magnetite relics. These samples exhibit magnetite-martite textural relationships similar to the ores from other Brazilian deposits located in the western low-strain domain (Hackspacher, 1979; Rosière, 1981; Rosière and Chemale,

1991), as well as in some Australian ores described by Morris (1980, 1983). Martite is developed along the (111) planes of magnetite or irregularly from the grain boundaries inward, resulting in a complex patchwork of anhedral porous hematite with magnetite relics and tiny inclusions with lower reflectivity under normal reflected light (hematite I, Fig. 3a). Most hematite grains, however, occur as nearly isometric granular crystals, usually <200 μm (hematite II, Fig. 3a-b, Table 1). They have curved to straight grain boundaries and are intergrown with hematite I, which appears as inclusion-bearing porous microdomains.

In the shear zone that cuts the massive ore two types of hematite occur: euhedral to subhedral tabular hematite crystals (hematite III, Fig. 3c-d, Table 1), which are dominant in microscopic dilational sites or occupying interstices between hematite II aggregates; and slim specularite platelets (Fig. 3e, Table 1) up to 500 μm long, oriented parallel or subparallel to the sharp boundaries of the shear.

The quartz vein is comprised of saccharoidal crystals (1–2 mm diam) that form a mosaic fabric enveloping ore fragments and distorted single crystals or aggregates of specularite. The vein has irregular borders and partially invades the ore along its banding and in the hinge zones of microfolds (Fig. 3f-h).

Analytical Procedures and Experimental Conditions

The use of infrared microscopy in the study of fluid inclusions in opaque minerals was first described by Campbell et al. (1984) and Campbell and Robinson Cook (1987). The methodology is described in Campbell et al. (1984), Richards and Kerrich (1993), Mancano and Campbell (1995), and Lüders and Ziemann (1999). The first application of infrared microscopy and microthermometry to the study of hematite was documented by Lüders et al. (1999).

Fluid inclusions and textural analyses in this study were conducted at the Fluid Inclusion laboratory (LIFM) of the

TABLE 1. Main Characteristics of the Iron Oxide Generations from the High-Grade Ore

Mineral	Microscopic features	Fluid inclusions	Fabric	Distribution in sample CO260
Magnetite	Irregularly shaped relics in hematite aggregates; intense martitization	Not transparent under infrared radiation	Originally as single idioblasts or as massive aggregates	Irregularly dispersed
Hematite I (Hm I)	Porous anhedral crystals; lobate to serrated grain boundaries	Numerous tiny (<1 μm), indistinct inclusions (solid inclusions or irregularities?)	Irregular to amoeboid; granoblastic fabric	Patches in the massive ore
Hematite II (Hm II)	Subhedral, nearly isometric, granular	(FI-1) generally spherical to elongated, two-phase; (FI-2) subrounded to tear drop-shaped, single phase with probable necking-down features	Polygonal, granoblastic fabric	Main component of the massive ore
Hematite II-III (Hm II-III)	Subhedral hybrid shapes (granular-tabular)	Two-phase, regular, partially elongated; restricted to the granular domain	Rare; together with Hm III	Interstitial in dilational zones
Hematite III (Hm III)	Euhedral to subhedral, tabular	Small, two-phase, aligned on the basal plane	Interstitial in the granoblastic fabric	Interstitial in dilational zones
Specularite	Platy	Two, three, and multiphase inclusions, negative crystal shape	Strong preferred orientation	Shear zone-hosted

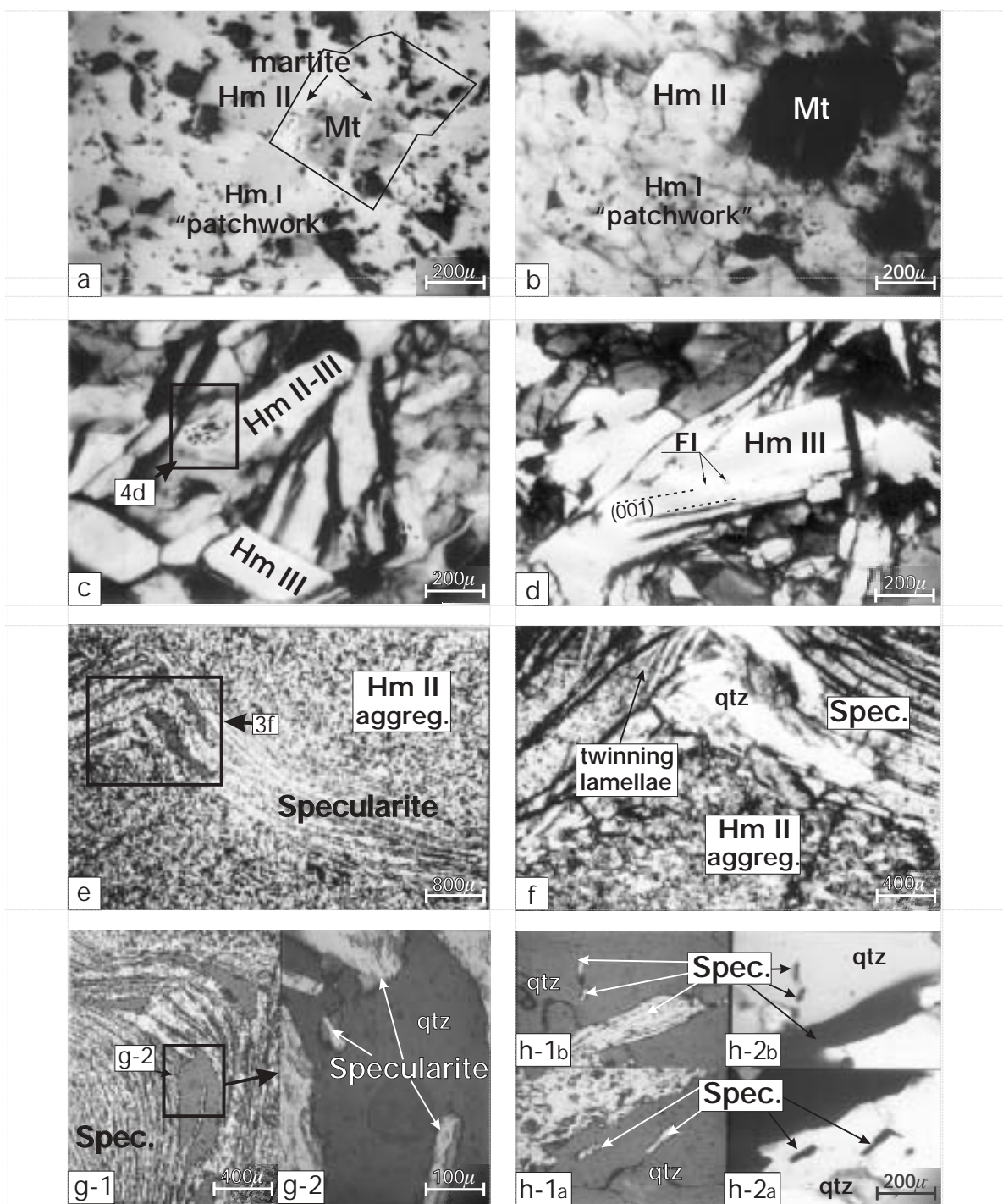


FIG. 3. Microscopic features of the analyzed ore types. (a). Porous microfabric of massive ore comprising crystals of anhedral porous hematite I (Hm I) and granular hematite II (Hm II) surrounding and enclosing martite with magnetite relic (Mt) (reflected light, partially crossed polarizers). (b). Same as (a) under infrared radiation. The original shape of incomplete martitized magnetite is recognized as the opaque mineral (Mt). Complete developed hematite crystals are transparent. (c). Aggregate of hematite II-III and hematite III. HmII-III is characterized by a tabular syntactic overgrowth on granular hematite. Relics of low-temperature and low-salinity fluid inclusions are depicted in the inset (infrared radiation). (d). Tabular crystal of hematite III (Hm III) with fluid inclusions (FI) aligned on the basal plane (001) (infrared radiation). (e). Microshear zone with oriented specularite crystals cutting aggregate of hematite II grains (Hm II). Inset depicts microfolded domain enlarged in Figure 3(f) (reflected light, partially crossed polarizers). (f). Enlargement of inset from (e), showing twinning lamellae in specularite plates and quartz (qtz) in the hinge zone of the microfold (infrared radiation). (g-1). Detail of microfold hinge zone. (g-2). Enlargement of inset from g-1, showing specularite plates enveloped by vein quartz (qtz) (plane reflected light). (h). Quartz (qtz) from vein domain envelops single plates and specularite aggregates (1a and b in plane reflected light; 2a and b in cross-polarized transmitted light).

Centro de Desenvolvimento de Tecnologia Nuclear (CDTN), Belo Horizonte, Brazil, using a Fluid Inc. heating/freezing system stage adapted to a Leica DMR-XP microscope. For calibration and precision tests commercially available synthetic standards were used. The microscope is equipped with a 100-W (12-V) transmitted-light illuminator, using halogen light bulbs as a source of visible and very near infrared radiation. The doubly polished sections studied were about 80 to 100 μm thick. The hematite crystals generally exhibit a good transparency in the very near infrared spectrum.

A Sony ExwaveHad black and white, very near-infrared camera and an Eletrophysics micronviewer model 7290-A IR camera, both coupled to a high-resolution monitor with a video graphic printer, provided the infrared images (Rios et al., 2000).

For the observation of thicker hematite sections, when the transparency under the regular halogen lamp was unsatisfactory, an infrared emission regulator with a 50-W 12-V Hosobuchi iodine-tungsten lamp was used. The infrared beam between the lamp bulb and the sample covered an overall distance of 40 cm and a maximum voltage of 5 V was applied during the measurements in order to avoid overheating of the sample.

During infrared analysis under room temperature (25°C) no temperature variation was registered in the sample, even in time intervals longer than 1 hr between measurements, inferring that the heat from the infrared source did not influence the microthermometric determinations. At temperatures higher than 300°C, a quick decline in the transparency of the hematite crystals could be observed.

Infrared microscopy of different hematite types

Infrared microscopy permits the observation of several remarkable features usually unseen under normal light. Under

near-infrared light, martite appears entirely opaque, and idiomorphic black magnetite ghosts (Mt, Fig. 3b) can be observed surrounded by hematite aggregates. This striking effect enables the recognition of the original shape and size of the magnetite crystals, despite oxidation that has almost totally obliterated the early fabric as seen under normal reflected light.

Under infrared light, it was also possible to recognize that some of the tabular hematite III crystals overgrow hematite II relics. The latter preserve two-phase fluid inclusions of the FI-1 type as described in the next section. This tabular hematite was classified separately as hematite II-III (Hm II-III, Fig 3c). Under infrared light, oriented specularite crystals display twinning lamellae (growth lamellae?) crisscrossing the plates (Fig. 3f). These features were not visible under polarized reflected light.

Fluid Inclusion Petrography and Microthermometry in Hematite Crystals

Martite and hematite I

Martite is opaque under infrared radiation and no fluid inclusions could be observed, although martite has a remarkable porosity under normal reflected light. Likewise, in the intergrown porous anhedral hematite I, it was not possible to identify fluid inclusions.

Hematite II

Although not all granular hematite II grains contain fluid inclusions, they are quite common and occur very noticeably as isolated inclusions with variable dimensions (5–50 μm). Two distinct groups can be distinguished (Table 2).

The first group (FI-1) comprises primary, two-phase inclusions, (L + V, fill ratio = 0.90–0.95). They are evenly

TABLE 2. Microthermometric Data from Primary Fluid Inclusions of Hematite and Quartz Crystals

Mineral phase	Primary fluid inclusions	Fill ratio ¹	Diam (μm)	$T_{\text{m(ice)}}$ (°C)	T_{h} (°C)	$T_{\text{m(CO}_2)}$ (°C)	$T_{\text{m(clathrate)}}$ (°C)	$T_{\text{h(CO}_2)}$ (°C)	Observations
Hematite II (Hm II)	(FI-1) Two-phase	0.90–0.95	5–50	–2.8 to –6.7 (18)	115 to 145 (18)	–	–	–	Decrepitated fluid inclusions (?)
	(FI-2) Single-phase	1.0	<4–50	NR	NR	–	–	–	
Hematite II-III (Hm II-III)	Two-phase	0.9	5–50	–2.0 to –2.5 (14)	120–145 (15)	–	–	–	Similar to (FI-1)
Hematite III (Hm III)	Two-phase	0.9–0.95	<8	–22.0 to –23.0 (4)	120–140 (5)	–	–	–	Solid phases are absent
Specularite	Two, three and multiphase	0.8–0.9	5 to 40	–10.0 to –24.5 (29)	140–205 (19)	–	–	–	Possible total dissolution of daughter crystals at 350°–400°C
Quartz	Two-phase	~0.8	<20		280–351 (42)	–57.0 (12)	5.0 to 6.0 (10)	26.0 to 28.0 (24)	Late fluids in relationship to specularite

Notes: $T_{\text{m(ice)}}$ = melting temperature of ice, T_{h} = homogenization temperature, $T_{\text{m(CO}_2)}$ = melting temperature of CO_2 , $T_{\text{m(clathrate)}}$ = melting temperature of clathrates; $T_{\text{h(CO}_2)}$ = homogenization temperature of CO_2 ; number in parentheses = number of measurements; NR = not recorded, – = no data

¹ $\text{vol}_{\text{liq}}/\text{vol}_{\text{total}}$

distributed through the entire grain, always in smaller crystals (on avg 80 μm) with sharp, straight boundaries, and near hexagonal sections, free of porous domains and magnetite relics. They are usually large (5–50 μm , Fig. 4a-b), nearly spherical or elongated, and lack any solid phases or daughter crystals. Freezing of the inclusions to -120°C caused no phase change and no clathrate formation, which suggests the lack of a CO_2 phase. Determination of the eutectic temperature (T_e) was not possible due to difficulties in the microscopic observation, but ice-melting temperatures ($T_{m(\text{ice})}$) were determined between -2.8° and -6.7°C , (salinities from 4.6 and 10.2 wt % NaCl equiv; Bodnar and Vityk, 1994). However, most of the measurements (14) varied from -2.8° and -3.0°C (Fig. 5a), corresponding to salinities from 4.6 to 4.9 wt percent NaCl equiv (Bodnar and Vityk, 1994). During heating runs, two-phase fluid inclusions homogenized (T_h) into liquid at temperatures of less than 145°C (Fig. 5b).

The second group (FI-2) is the most common and consists of single-phase inclusions that occur alone or in groups concentrated in the core of larger crystals (usually $>100 \mu\text{m}$), generally surrounded by a clear, inclusion-free rim (Fig. 4c-). They have subrounded to teardrop shapes with sizes from 4 to 50 μm and strong relief. Some of the larger inclusions are partially constricted (probably evidence of necking down) and surrounded by smaller inclusions (Fig. 4c-2). All of the analyzed inclusions had apparently leaked and were probably empty.

Hematite II-III

In the tabular-granular hematite II-III crystals, primary fluid inclusions are present only in the granular domain (Fig. 4d, Table 2). They are two-phase inclusions (L + V), with variable sizes (5–50 μm). Solid phases are absent, and the fill ratio is constant (~ 0.9). Microthermometric determinations indicate a behavior similar to the FI-1 inclusions observed in hematite II crystals. The $T_{m(\text{ice})}$ is -2.0° to -2.5°C (corresponding to salinities from 3.39–4.18 wt % NaCl equiv; Bodnar and Vityk, 1994), and T_h in the liquid phase varies from 120° to 145°C . With continued heating all inclusions decrepitated at 345° to 350°C . This is thought to be due to weakening of the crystal structure during subsequent shearing (see below). Determination of the eutectic temperature (T_e) was not possible due to optical difficulties in the microscopic observation.

Hematite III

Idiomorphic tabular crystals of hematite III contain minute ($<8 \mu\text{m}$), two-phase (L + V) fluid inclusions of primary origin, some of them as negative crystals (Fig. 4e, Table 2). Most of the inclusions are oriented along growth planes, probably parallel to the basal pinacoid. During freezing and heating $T_{m(\text{ice})}$ was determined in the range -22° to -23°C , and T_h was between 120° and 140°C . Determination of the eutectic temperature (T_e) was not possible due to optical difficulties in the microscopic observation.

Specularite

Fluid inclusions in specularite are primary, usually with negative crystal shape, smaller than 40 μm , and composed of two, three, and rarely four phases (L + V + S + S, fill ratio = 0.8–0.9; Fig. 4f-g, Table 2). Solid phases are ubiquitous but

always very small ($<10\%$ of the total volume of the fluid inclusions) and never exhibit a definitive geometric shape. Fluid inclusions are concentrated along the basal planes, and in slightly deformed crystals they locally have a sigmoidal shape (Fig. 4f). The eutectic temperatures (T_e) in some inclusions range between -60° and -50°C , suggesting the presence of Ca^{2+} , Fe^{2+} , or Mg^{2+} in the solution. The $T_{m(\text{ice})}$ values varied between -10.0° and -24.5°C (Fig. 5a), and most of the values concentrated in the narrow range of -19.0° and -24.5°C . In freezing and heating runs, no development of clathrates or melting or homogenization of CO_2 was observed, suggesting that CO_2 is not present in these inclusions. Homogenization temperatures (T_h) in the liquid phase ranged from 140° to 205°C (Fig. 5b). At 300°C the solid phase would commonly begin to dissolve, and above 300° to 350°C optical definition rapidly decreased and no detailed observation (final melting temperature) could be made. The total dissolution of the solids at a temperature higher than 350°C together with the determined $T_{m(\text{ice})}$ suggest a high salinity, above 30 wt percent NaCl equiv (Bodnar and Vityk, 1994).

Quartz

Quartz contains two main types of fluid inclusions. The first is represented by primary and small ($<20 \mu\text{m}$), three-phase, aqueous carbonic inclusions ($\text{L}_{\text{H}_2\text{O}} + \text{L}_{\text{CO}_2} + \text{V}_{\text{CO}_2}$) at 25°C , with polygonal shapes (Fig. 4h). During freezing runs, T_m (CO_2) was determined at -57°C , suggesting the presence of other components in the carbonic phase. Raman spectra measurements in these fluid inclusions indicated the possible presence of traces of N_2 (Manduca et al., 2001). The clathrate melting temperature ($T_{m(\text{clathrate})}$) varied between 5° and 6°C , indicating salinities close to 8 wt percent NaCl equiv (Collins, 1979). CO_2 homogenization to the liquid phase occurred between 26° and 28°C . The temperature of total homogenization into the liquid varied between 280° and 351°C , with modal values at 330° to 340°C (Fig. 5c).

The second type of fluid inclusion is less common and paragenetically late (secondary fluid inclusions). They occur aligned along fracture planes, usually close or crosscutting the grain borders. They are aqueous two-phase inclusions (L + V) without carbonic phases (no development of clathrates or melting or homogenization of CO_2 was observed in freezing and heating runs), and they have salinities between 6 and 7.8 wt percent NaCl equiv. During heating they homogenized in the liquid phase between 169° and 224°C (Fig. 5c).

Discussion

Evidence from petrographic analysis and fluid inclusions studies indicate that martitization and formation of hematite I, and crystallization of hematite II, hematite III, and specularite occurred during, at least, three distinct stages involving different hydrothermal fluids, metamorphism and deformation processes (Figs. 6-7) as discussed below.

An initial low-salinity fluid was possibly responsible for the development of an originally magnetite-rich ore, in a way similar to that proposed by Taylor et al. (2001), followed by oxidation to hematite I and upgrading during a subsequent hydrothermal event. Post-tectonic recrystallization contributed to grain growth and to the development of a granoblastic

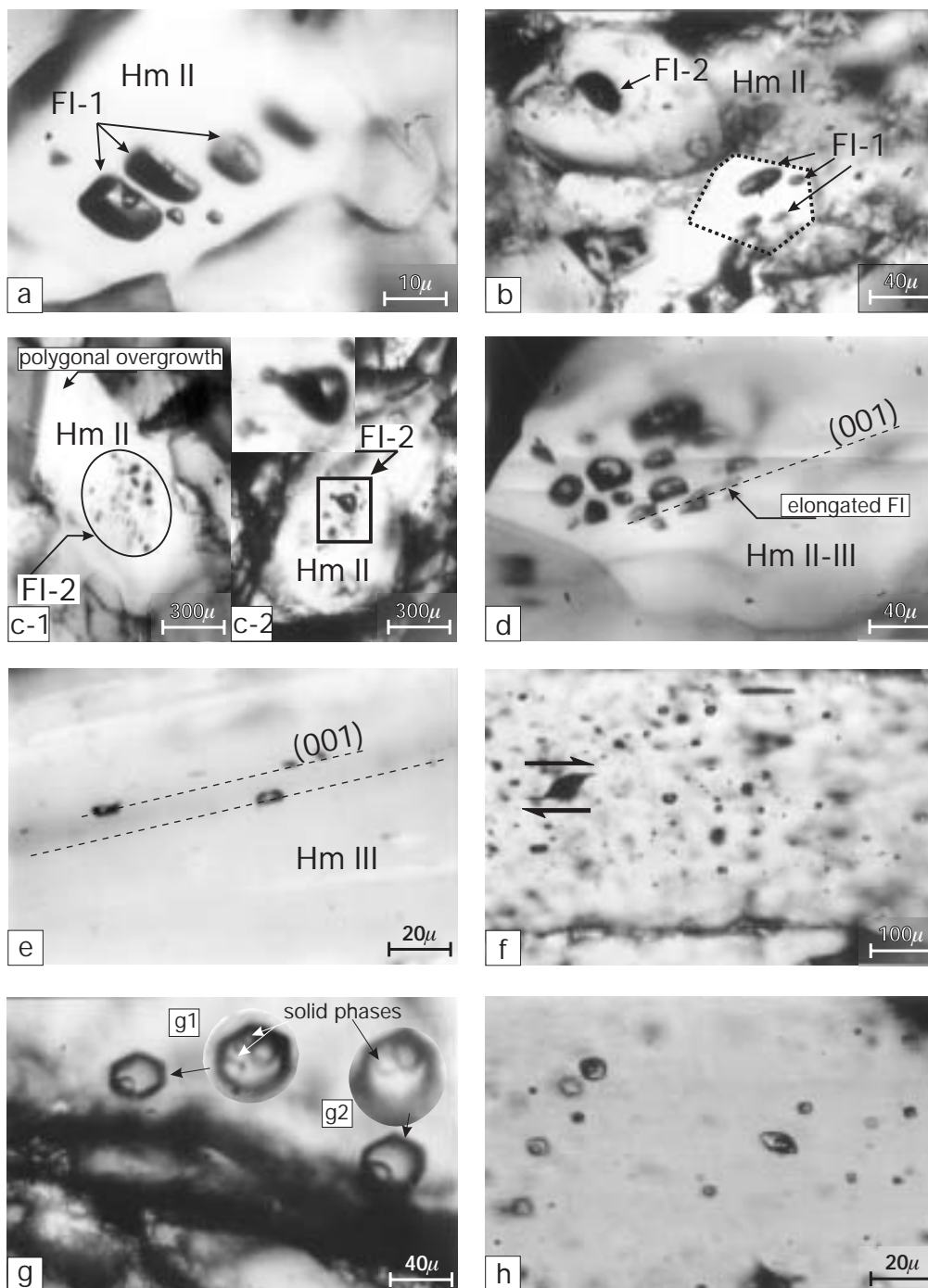


FIG. 4. Fluid inclusions in hematite, all under infrared radiation; in quartz, under normal light. (a). Large, two-phase aqueous fluid inclusions (FI-1) in granular hematite II. Hematite II crystal exhibits birefringence under infrared light with the formation of a double-image in some FI-1 fluid inclusions. (b). FI-1-FI-2 fluid inclusions in neighboring hematite II crystals that compose the granoblastic fabric. (c-1). Single-phase fluid inclusions (FI-2) in core domain of granular hematite (Hm II). Borders are clear and fluid inclusion free. (c-2). Larger balloon-shaped single-phase fluid inclusion surrounded by smaller inclusions (FI-2) in Hm II crystal. Inset shows enlargement of the balloon-shaped fluid inclusions and evidence of probable necking down. (d). Enlargement of inset from Figure 3(c), showing primary two-phase fluid inclusions typical of Hm II crystals, enclosed in an Hm II-III grain. Some of the inclusions are elongated parallel to the basal plane and deprecipitated at 345° to 350°C. (e). Two-phase inclusions oriented parallel to the basal plane in hematite III (Hm III) crystal. (f). Primary fluid inclusion in specularite crystal. The sigmoidal shape is interpreted to be due to gliding along the basal plane. (g). Large fluid inclusions with hexagonal shape in specularite. The fluid inclusions in the left-hand side contain a small solid saturation phase. Insets g1 and g2 are enlargements showing solid inclusions that formed after heating. In g1 two solid phases formed after heating to 400°C and subsequent cooling. In g2 a single solid phase formed after heating and cooling. (h). Primary aqueous carbonic fluid inclusions in quartz at 25°C. $T_{m(ice)} = 16.6^{\circ}\text{C}$ and $T_{h(total)} = 149^{\circ}\text{C}$.

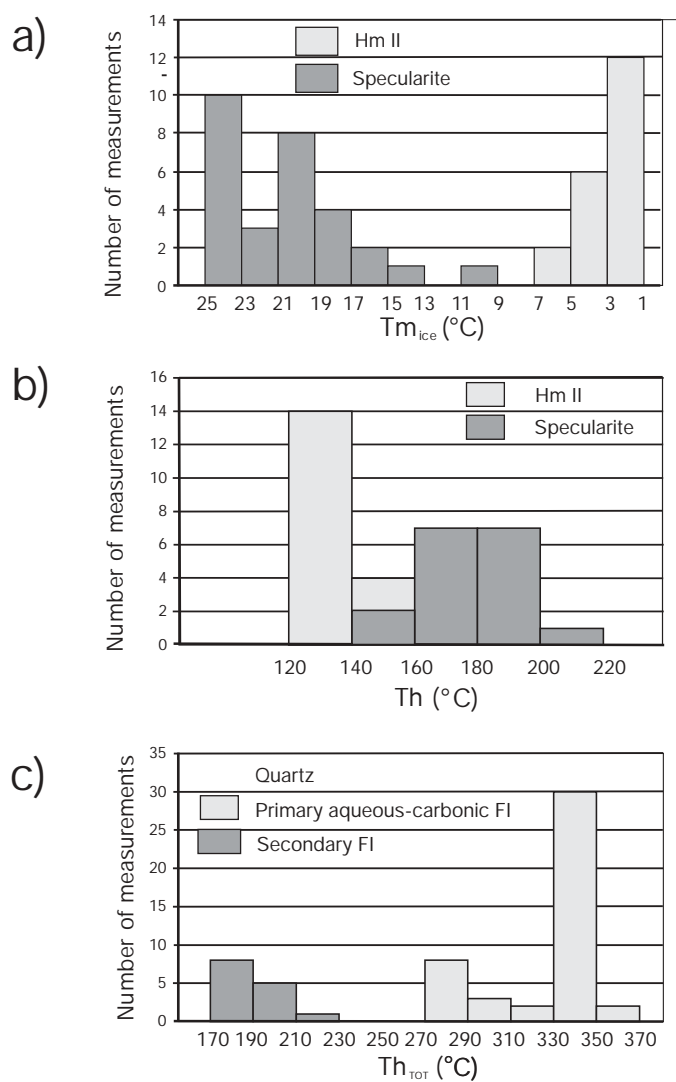


FIG. 5. Histograms of microthermometric data. (a). Final ice melting temperature $T_{m(ice)}$ for fluid inclusions in hematite II (Hm II) and specularite. (b). Homogenization temperature (T_h) of primary fluid inclusions for hematite II (Hm II) and specularite. (c). Temperature of total homogenization $T_{h(tot)}$ of primary aqueous carbonic fluid inclusions and homogenization temperature of late, secondary, fluid inclusions in vein quartz.

fabric. A high-salinity hydrothermal event was responsible for the formation of younger generations of hematite crystals related to shear zones.

Origin of hematite I and II

Earlier studies of the textural relationships between magnetite, martite, and the granular and anhedral hematite grains showed that both hematite I and II developed at least in part at the expense of magnetite (see also Hackspacher 1979; Rosière, 1981) and represent only different degrees of recrystallization. The present work reveals further details of a more complex sequence of postmagnetite events. Oxidation of magnetite and inversion to hematite results in a volume decrease (cf. Davis et al., 1968; Morris, 1983), producing an

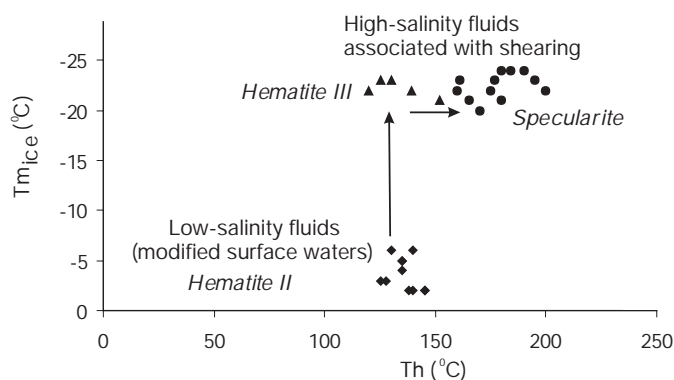


FIG. 6. Plot of ice-melting temperatures vs. temperatures of homogenization, illustrating the evolution of the fluids involved in the oxidation and mineralization of the high-grade iron orebody in the Conceição deposit. (♦) = two-phase fluid inclusions (FI-1) from the core of hematite II (●) = fluid inclusions from Hm III, (▲) = daughter crystals-bearing fluid inclusions from specularite. Tabular hematite III crystals do not contain daughter crystals, suggesting an increase in the salinity during formation of specularite.

aggregate of porous anhedral hematite (hematite I) with inclusions of magnetite relics and several internal irregularities that could not be identified.

Hematite II, granular crystals, which occur intergrown with martite and hematite I, formed by the partial recrystallization of the ore during metamorphism. They locally contain magnetite relics, indicating their formation by recrystallization of hematite I. Although most of the grains are now free of fluid inclusions, many of them also contain large two- and single-phase inclusions. The single-phase inclusions (FI-2) are interpreted as the product of necking down and leaking of pre-existing fluid inclusions during metamorphism, culminating with a multitude of empty inclusions scattered in the core of many crystals. The two-phase fluid inclusions (FI-1) are thought to be related to a low-temperature hydrothermal event, involving low- to medium-salinity fluids that were responsible for the formation of new crystals of hematite II.

Origin of transitional hematite II-III, hematite III, and specularite

The textural relationship and fluid inclusion data from tabular hematite III and platy specularite crystals indicate that both morphological types developed later than the hematite II (Rosière et al, 2001; this study). The two occur in wedge-shaped shear zones that cut the massive, granoblastic ore and were formed in the presence of a high-salinity fluid that was distinctly different from the earlier, low-temperature and low- to medium-salinity fluid (Fig. 6).

Tabular-shaped hematite III crystals have grown mostly interstitial to the granoblastic hematite II aggregates but also in isolated dilational sites and as veins with sharp to fuzzy boundaries in the walls of the shear zone. Their fluid inclusions have high salinity and relatively low homogenization temperatures (ca. 140°C). Hematite III may also overgrow hematite II, forming the hematite II-III transitional type (Hm II-III, Fig. 3c). These composite grains still contain relic primary fluid inclusions (Fig. 4d) inherited from the original hematite II. They have the same T_h and $T_{m(ice)}$ as FI-1 fluid inclusions but

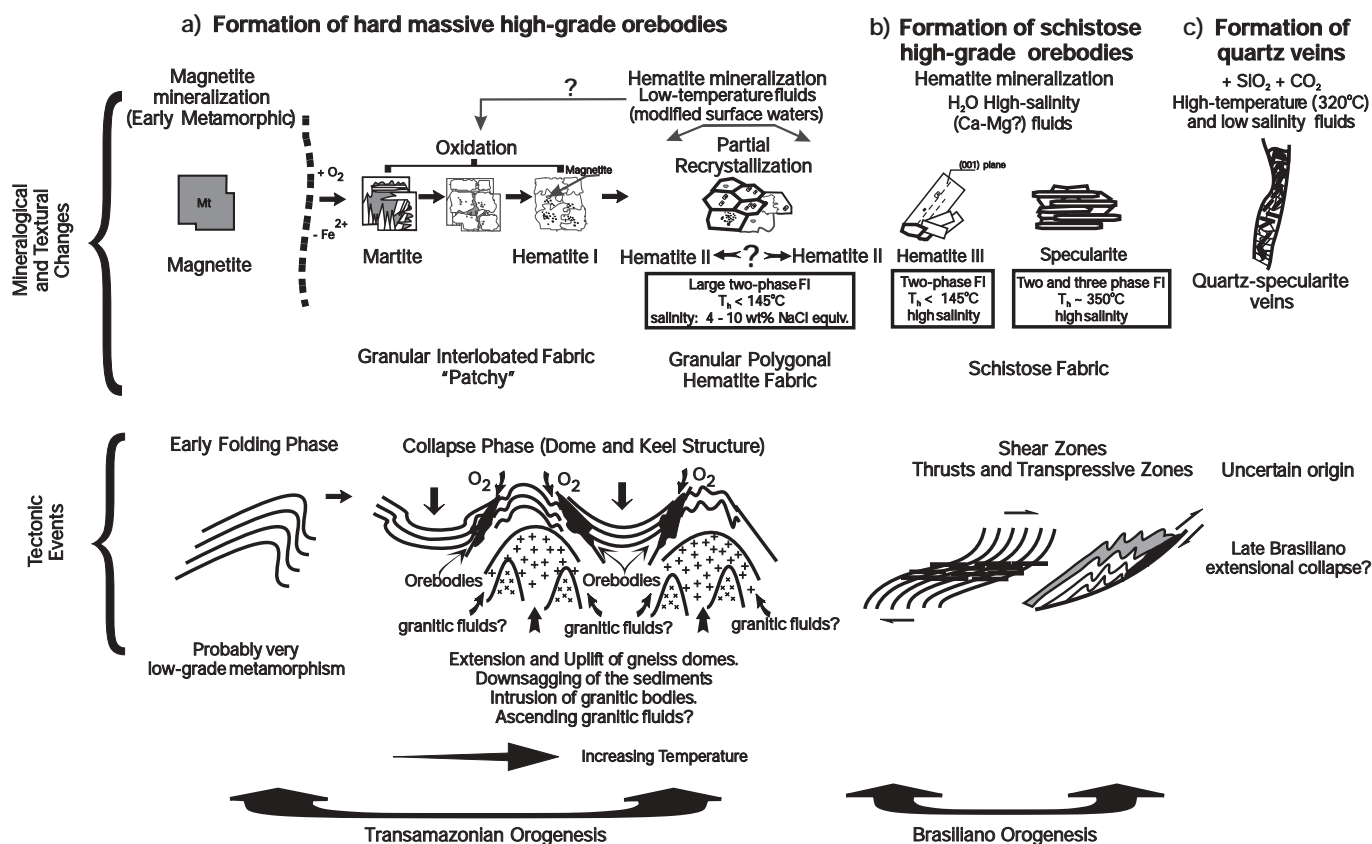


FIG. 7. Conceptual model for the generation of the different types of hematite in high-grade iron ore from the Quadrilátero Ferrífero. The mineralogical changes in the ore are shown schematically in the upper part of the diagram. The corresponding tectonic events during the Transamazonian event developed in two distinct stages. Magnetite mineralization consists of blasts probably formed in the early stages of the event during the first folding phase. Hematite mineralization: occurred during the collapse stage, coincident with the development of dome-and-keel regional structures and partial uplift of the sequence. Progressive regional increase of temperature, probably due to the juxtaposition of the cooler supracrustal rocks and the relatively hot uplifted basement and/or intrusion of granitic plutons, produced a granoblastic fabric of hematite grains with relic magnetite and locally preserved primary fluid inclusions. Low-temperature meteoric fluids penetrated along major extensional faults, with precipitation of hematite crystals rich in fluid inclusions. Similar fluids might also have been responsible for the earlier oxidation of magnetite (martitization) and formation of the porous hematite aggregates (hematite I). (b). Formation of schistose high-grade iron orebodies during the Brasillano event involving high-temperature fluids. The main mineralogical changes developed along shear zones. High-salinity fluids caused the growth of idiomorphic, tabular crystals of hematite III and promoted ductile deformation of the existing hematite grains to produce long oriented specularite platelets that define the schistosity. Quartz from the iron formation was also probably leached at this stage with the development of schistose high-grade ore and iron-rich itabirite bodies. (c). Late quartz veins formed from high-temperature, low-salinity fluids and cut across the orebodies. The veins incorporate massive and schistose ore fragments. They are unrelated to the iron mineralization and could have formed during the Brasillano collapse phase.

decrepitate between 345° and 350°C, a feature that is not observed in the FI-1 fluid inclusions in hematite II. The decrepitation of these inclusions is interpreted as resulting from the structural weakening of the crystals during shearing.

On the other hand, specularite formed at higher temperatures in the central domain of the shear zones where penetration of fluids was enhanced. The lowest temperature of formation of specularite, inferred from the partial dissolution of the daughter crystals, is about 350°C, which is much higher than the homogenization temperature for aqueous inclusions trapped both in hematite II and III.

Specularite may form by crystal-plastic deformation of hematite, through dislocation glide on the basal plane, as

discussed by Rosière et al. (2001) and determined experimentally by Siemes et al. (2003), or by fluid-assisted diffusion processes (Lagoeiro, 1998). In the Conceição samples, basal gliding on specularite is suggested by the presence of sigmoidal inclusions (Fig. 4f) aligned parallel to the trace of the (001) plane, although the prevailing temperatures (ca. 350°C) were much lower than the experimental values of 600°C from Siemes et al. (2003).

Both hematite III and specularite were apparently formed from similar high-salinity fluids at different stages in the evolution of the shear zones and represent the third and last hypogene mineralization event. Hematite III precipitated in the early stages, at low temperature, during the opening of

dilatational gashes without the development of a preferred orientation, and overgrowing hematite II grains. Specularite formed at higher temperature and at higher strain.

Relationship to quartz veins

The quartz veins from the analyzed samples cut across the metamorphic schistosity (S_1) or interfinger with the banded microstructure of the hematite ores. They envelop all the early minerals, including specularite plates and are the product of late, aqueous carbonic hydrothermal fluids of low salinity (less than 8 wt % NaCl equiv), with total homogenization temperatures of the fluid inclusions of approximately 330°C. These fluids are of uncertain age and origin and did not participate in oxidation of magnetite or Fe mineralization processes.

Metamorphism and preservation of low-temperature fluid inclusions

Although metamorphism produced a general granoblastic fabric in the massive ores, many granular crystals have preserved magnetite and martite relics in their cores. Some of the hematite II grains contain low-temperature, two-phase fluid inclusions (FI-1) and others contain probably empty or necked inclusions (FI-2). The low-temperature two-phase inclusions are thought to be relics that have been unaffected by metamorphism. This interpretation is supported by the presence of relict magnetite and martite in the core of some crystals. Regardless of their size, the FI-1 inclusions in the hematite II crystals show no indication of fluid loss by leakage or decrepitation or any metastability during microthermometric measurements, including heating up to 350°C and subsequent cooling. The fill ratio was constant for all analyzed inclusions, and both the fill ratios and homogenization temperatures remained constant, even with repeated heating and cooling. These observations suggest that some of the hematite was quite stable under the metamorphic conditions that prevailed in this part of the Quadrilátero Ferrífero. Marshall et al. (2001) pointed out that there is no clear answer to the problem of the stability of fluid inclusions during metamorphism, and there are many examples of fluid inclusions studies of amphibolite facies gold deposits that contain both completely recrystallized quartz with homogenized fluid inclusion populations and relatively undeformed quartz with undisturbed fluid inclusion populations (e.g., including a population of several different types, different L/V ratios, and different homogenization temperatures). Microscopic and field observations also suggest that hematite may be more stable than quartz under certain conditions of metamorphism (e.g., Hippert et al., 2001; Siemes et al., 2003).

Conclusions

The analysis of the textural relationships and fluid inclusions preserved in the Conceição ores support a provisional genetic model for the development of two types of high-grade orebodies: hard massive, partially concordant bodies, and tabular, schistose bodies controlled by shear zones (see also Fig. 7). Mineralization developed in several recurrent stages, with the participation of fluids of different characteristics and origin, including both hypogene and supergene processes.

Magnetite growth represents an early (probably initial) mineralization stage (Fig. 7), but its age cannot be precisely

determined yet. This mineral is ubiquitous in the iron formations and high-grade bodies of the Quadrilátero Ferrífero, either as relics or as the main component in the extreme western part of the region. We suggest that in the early contractional stage of the Transamazonian orogeny (ca. 2.1–2.0 Ga; Alkmim and Marshak, 1998) reduced metamorphic fluids, together with connate water, were responsible for the pervasive magnetite mineralization similar to the model proposed by Taylor et al. (2001) for the Tom Price deposit in Western Australia. The folds of this phase of deformation are of flexural or flexural slip type, commonly with disharmonic to polyharmonic profiles, and did not develop a pervasive axial-planar cleavage (Rosière et al., 1993, 1996; Hippert and Davis, 2000).

Hematite I formed from martite following the oxidation of the magnetite (Rosière, 1981; Rosière and Chemale, 1991; Rosière et al., 2001), whereas much of the hematite II grains grew from low-temperature and low- to medium-salinity hydrothermal fluids during a second episode of mineralization (Fig. 7). These fluids are interpreted to have been of meteoric origin (Fig. 7a), moving downward from the surface along normal faults and fractures during progressive uplift and extension of the crust at the end of the Transamazonian event. Such fluids may have been responsible for oxidation of the banded iron formations in the entire Quadrilátero Ferrífero district, but the high-grade bodies were developed only at sites of greater permeability such as fold hinges. Faults that controlled the mineralization have not been positively identified in the Conceição deposit, owing to overprinting by structures developed during subsequent shortening, but the main orebody occurs within a relict Transamazonian structure (i.e., refolded F_1 hinge zone of the Itabira synclinorium; Fig. 2).

The peak of the regional metamorphism in the Quadrilátero Ferrífero probably occurred during the Transamazonian extensional tectonism (Alkmim and Marshak, 1998) caused by the juxtaposition of hot basement and cooler supracrustal rocks, producing a granoblastic fabric in all rock assemblages of the Minas Supergroup. During crustal extension, ascending plutonic rocks (Noce, 1995) most likely caused additional recrystallization.

Syndeformational growth of idiomorphic, tabular hematite III and of specularite plates occurred during the later Brasiliano/PanAfrican orogeny in domains of intense deformation, with the development of a pervasive schistosity, mainly in the eastern part of the Quadrilátero Ferrífero (Chemale et al., 1994). High-salinity (probably more than 20 wt % NaCl equiv) fluids penetrated along shear zones in its early stages, causing the precipitation of hematite III (Figs. 6–7) in microscopic dilatational sites. Similar but higher temperature (~350°C) and high-salinity fluids assisted deformation by facilitating hematite basal gliding, forming platy hematite crystals (specularite). SiO_2 from the iron formation must also have been leached by these fluids, and cations such as Ca^{2+} , Fe^{2+} , and Mg^{2+} were probably added to the system, possibly derived from dolomitic rocks at depth (Fig. 2). The combination of these factors produced the shear zone-related, high-grade tabular orebodies (Rosière et al., 2002). Although the relationship between the microshear zone, which hosts the sample analyzed in this study, and the regional structure is not clear, it is suggested that the relatively high grade of the presently mined sheared itabirite from the deposits in the

Itabira synclinorium is a result of this third, shear-related, mineralization event (Fig. 7).

A similar model may apply to other deposits of the Quadrilátero Ferrífero, particularly in the western low-strain domain, where the early Transamazonian structures are better preserved. In this region, the most significant high-grade massive bodies are located in zones of internal folding, especially close to the contact with the uplifted gneiss basement and granitic bodies. In the eastern domain, weathered, schistose and sheared itabirite bodies have developed even in the absence of an oxidized magnetite protore and may represent an important exploration target.

Acknowledgments

We wish to express our thanks to the FAPEMIG Foundation (Process CRA 175/02 to FJR) and to the research staff of EC1-CDTN, especially K. Fuzikawa, J. V. Alves, J. M. Correia-Neves, W. Macedo, and E. Costa. A. Matias is thanked for the excellence of the double-polished chips of hematite. Our thanks are also extended to CVRD, especially E. M. Resende de Souza, M. L. Vidigal Guimarães, and E. Caldeira Leite for generously supplying the samples and sharing useful information. Thanks to W. Tito Soares from the Laboratório de Microscopia Eletrônica e Microanálises (UFMG-CDTN-FAPEMIG CEX 1074/95). C. A. Rosière particularly thanks the CNPq (Brazilian National Research Council) for the grant, CAPES, FINEP/PADCT, and DAAD for all the previous support. Special thanks are due to H. Quade, the former supervisor of CAR for introducing him and other students of the Clausthaler Group to the problems of iron ore genesis and L. Lobato, N. Beukes, M. Barley, B. Simonson, J. Gutzmer, and C. A. Spier for the fruitful discussions. Many thanks are indebted to V. Lüders for the valuable explanations about methodology and technical details of the infrared equipment and to A. Campbell for his comments on infrared radiation sources. Finally, thanks are also due to M. Hannington (editor of *Economic Geology*), A. Cabral, and particularly to S. Hagemann whose valuable review and suggestions contributed considerably to the improvement of the paper.

November 20, 2001; December 16, 2003

REFERENCES

- Alkmim, F.F., and Marshak, S., 1998, Transamazonian orogeny in the Southern São Francisco craton region, Minas Gerais, Brazil: Evidence for Paleoproterozoic collision and collapse in the Quadrilátero Ferrífero: *Precambrian Research*, v. 90, p. 29–58.
- Almeida, F.F.M., 1977, O Craton de São Francisco: *Revista Brasileira de Geociências*, v. 7, p. 349–364.
- Baars, F., and Rosière, C.A., 1997, Geological map of the Quadrilátero Ferrífero, in DeWitt, M.J., and Ashwal, L.A., eds., *Greenstone belts: Oxford Monographs on Geology and Geophysics Series*, Oxford University Press, p. 529–557.
- Babinski, M., Chemale, F., Jr., and Van Schmus, W.R., 1995, The Pb/Pb age of Minas Supergroup carbonate rocks, Quadrilátero Ferrífero, Brazil, and its implications to the correlation with BIFs from South Africa and Australia: *Precambrian Research*, v. 72, p. 235–245.
- Barley, M.E., Pickard, A.L., Hagemann, S.G., and Folkert, S.L., 1999, Hydrothermal origin for the 2 billion year old Mount Tom Price giant iron ore deposit, Hamersley province, Western Australia: *Mineralium Deposita*, v. 34, p. 784–789.
- Beukes, N.J., 1984, Sedimentology of the Kuruman and Griquatown iron formations, Transvaal Supergroup, Griqualand West, South Africa: *Precambrian Research*, v. 24, p. 47–84.
- Bodnar, R.J., and Vityk, M.O., 1994, Interpretation of microthermometric data for H₂O-NaCl fluid inclusions, in De Vivo, B., and Frezzotti, M., eds., *Fluid inclusions in minerals: Methods and applications*: Blacksburg, Virginia, Virginia Tech, p.117–130.
- Campbell, A.R., and Robinson Cook, S., 1987, Infrared fluid inclusion microthermometry on coexisting wolframite and quartz: *ECONOMIC GEOLOGY*, v. 82, p. 1640–1645.
- Campbell, A.R., Hackbarth, C.J., Plumlee, G.S., and Petersen, U., 1984, Internal features of ore minerals seen with the infrared microscope: *ECONOMIC GEOLOGY*, v. 79, p. 1387–1392.
- Chemale, F., Jr., 1987, Tektonische, lagerstättenkundliche und petrographische Untersuchungen im Eisenerzrevier Itabira, Minas Gerais, Brasilien: Unpublished Ph.D. thesis, Clausthal-Zellerfeld, Germany, Technische Universität Clausthal, 140 p.
- Chemale, F., Jr., Quade, H., and Santana, F.C., 1987, Economic and structural geology of the Itabira iron district, Minas Gerais, Brazil: *Zentralblatt für Geologie und Paläontologie*, v. 6, p. 743–752.
- Chemale, F., Jr., Rosière, C.A., and Endo, I., 1994, The tectonic evolution of the Quadrilátero Ferrífero, Minas Gerais, Brazil: *Precambrian Research*, v. 65, p. 25–54.
- Chemale, F., Jr., Quade, H., and Van Schmus, W.R., 1997, Petrography, geochemistry and geochronology of the Borrachudo and Santa Barbara metagranites, Quadrilátero Ferrífero, Brazil: *Zentralblatt für Geologie und Paläontologie*, part I, no. 3-6, p. 739–750.
- Collins, P.L.F., 1979, Gas hydrates in CO₂-bearing fluid inclusions and the use of freezing data for estimating of salinity: *ECONOMIC GEOLOGY*, v. 74, p. 1435–1444.
- Davis, B.L., Rapp, G., Jr., and Walawender, M.J., 1968, Fabric and structural characteristics of the martitization process: *American Journal of Science*, v. 266, p. 482–496.
- Dorr, J.V.N., II, 1964, Supergene iron ores of Minas Gerais, Brazil: *ECONOMIC GEOLOGY*, v. 59, p. 1203–1240.
- 1965, Nature and origin of the high-grade hematite ores of Minas Gerais, Brazil: *ECONOMIC GEOLOGY*, v. 60, p. 1–46.
- 1969, Physiographic, stratigraphic and structural development of the Quadrilátero Ferrífero, Minas Gerais: *U.S. Geological Survey Professional Paper 641-A*, 110 p.
- Dorr, J.V.N., II, and Barbosa, A.L.M., 1963, Geology and ore deposits of the Itabira district, Minas Gerais, Brazil: *U.S. Geological Survey Professional Paper 341-C*, 110 p.
- Gruner, J.W., 1924, Contributions to the geology of the Mesabi Range, with special reference to the magnetites of the iron-bearing formations west of the Mesaba: *Minnesota Geological Survey Bulletin 19*, 71 p.
- 1926, Magnetite-martite-hematite: *ECONOMIC GEOLOGY*, v. 21, p. 375–393.
- 1930a, Hydrothermal oxidation and leaching experiments: Their bearing on the origin of the Lake Superior hematite-limonite ores: *ECONOMIC GEOLOGY*, v. 25, pt. I, p. 697–719.
- 1930b, Hydrothermal oxidation and leaching experiments: Their bearing on the origin of the Lake Superior hematite-limonite ores: *ECONOMIC GEOLOGY*, v.25, pt. II, p. 837–867.
- 1937, Hydrothermal leaching of iron ores of the Lake Superior type—a modified theory: *ECONOMIC GEOLOGY*, v. 32, p. 121–130.
- Guba, I., 1982, Tektonik, Texturen und Mineralogie der präkambrischen Eisenerze und Nebengesteinsserien der Lagerstätten Morro Agudo im NE des Quadrilátero Ferrífero/Minas Gerais, Brasilien: Unpublished Ph.D. thesis, T. U. Clausthal, 342 p.
- Guild, P.W., 1953, Iron deposits of the Congonhas district, Minas Gerais, Brazil: *ECONOMIC GEOLOGY*, v. 48, p. 639–676.
- 1957, Geology and mineral resources of the Congonhas district, Minas Gerais, Brazil: *U.S. Geological Survey Professional Paper 290*, 90 p.
- Hackspacher, P.C., 1979, Strukturelle und texturale Untersuchungen zur internen Deformation des Eisenreicherzkörpers der Grube "Águas Claras" bei Belo Horizonte, Minas Gerais, Brasilien: *Geologische Abhandlungen*, v. 34, 164 p.
- Hagemann, S.G., Barley, M.E., Folkert, S.L., Yardley, B.W., and Banks, D.A., 1999, A hydrothermal origin for the giant BIF-hosted Tom Price iron ore deposit, in Stanley et al., eds. *Mineral deposits: Processes to processing*: Rotterdam, Balkema, p. 41–44.
- Herz, N., 1978, Metamorphic rocks of the Quadrilátero Ferrífero, Minas Gerais, Brazil: *U.S. Geological Survey Professional Paper 641C*, 78 p.
- Hippert, J., and Davis, B., 2000, Dome emplacement and formation of kilometer-scale synclines in a granite-greenstone terrain (Quadrilátero Ferrífero, southeastern Brazil): *Precambrian Research*, v. 102, p. 99–121.

- Hippertt, J., Lana, C., and Takeshita, T., 2001, Deformation partitioning during folding of banded iron formation: *Journal of Structural Geology*, v. 23, p. 819–834.
- Hoefs, J., Müller, G., and Schuster, A., 1982, Polymetamorphic relations in iron ores from the Iron Quadrangle, Brazil: The correlation of oxygen isotope variations with deformation history: *Contributions to Mineralogy and Petrology*, v. 79, p. 241–251.
- Kullerud, G., Donnay, G., and Donnay, J.D.H., 1969, Omission solid solution in magnetite: Kenotetrahedral magnetite: *Zeitschrift der Kristallographie*, v. 128, p. 1–17.
- Lagoeiro, L.E., 1998, Transformation of magnetite to hematite and its influence on the dissolution of iron oxide minerals: *Journal of Metamorphic Geology*, v. 16, p. 415–423.
- Leith, C.K., 1903, The Mesabi iron-bearing district of Minnesota: U.S. Geological Survey Monograph 43, 316 p.
- Leith, C.K., Lund, R.J., and Leith, A., 1935, Pre-Cambrian rocks of the Lake Superior region: U.S. Geological Survey Professional Paper 84, 34 p.
- Lüders, V., and Ziemann, M., 1999, Possibilities and limits of infrared light microthermometry applied to studies of pyrite-hosted fluid inclusions: *Chemical Geology*, v. 154, p. 169–178.
- Lüders, V., Gutzmer, J., and Beukes, N.J., 1999, Fluid inclusion studies in co-genetic hematite, hausmannite, and gangue minerals from high-grade manganese ores in the Kalahari manganese field, South Africa: *ECONOMIC GEOLOGY*, v. 94, p. 589–596.
- Machado, N., and Carneiro, M.A., 1992, U-Pb evidence of the Late Archean tectono-thermal activity in the southern São Francisco shield, Brazil: *Canadian Journal of Earth Sciences*, v. 29, p. 2341–2346.
- Machado, N., Noce, C.M., Belo de Oliveira, O.A., and Ladeira, E.A., 1989, Evolução Geológica do Quadrilátero Ferrífero no Arqueano e Proterozóico Inferior com Base em Geocronologia U-Pb: Anais do V Simpósio de Geologia de Minas Gerais, Belo Horizonte: Boletim da Sociedade Brasileira de Geologia, Núcleo de Minas Gerais, v. 10, p. 1–4.
- Machado, N., Noce, C.M., Ladeira, E.A., and Belo de Oliveira, O.A., 1992, U-Pb geochronology of Archean magmatism and Proterozoic metamorphism in the Quadrilátero Ferrífero, southern São Francisco craton, Brazil: *Geological Society of America Bulletin*, v. 104, p. 1221–1227.
- Mancano, D.P., and Campbell, A.R., 1995, Microthermometry of enargite hosted fluid inclusions from Lepanto, Phillipines, high sulfidation Cu-Au deposit: *Geochimica et Cosmochimica Acta*, v. 59, p. 3909–3916.
- Manduca L.G., Rosière, C.A., Alves, J.V., Rios, F.J., Fuzikawa, K., and Correa Neves, J.M., 2000, Estudo de inclusões fluidas de cristais de quartzo das formações ferríferas bandadas da mina de Conceição, Quadrilátero Ferrífero [abs.]: Proceedings of the IX Semana de Iniciação Científica, Universidade Federal de Minas Gerais, Belo Horizonte, p. 269.
- Marshak, S., Alkmim, F.F., and Jordt-Evangelista, H., 1992, Proterozoic crustal extension and generation of dome and keel structure in the Archean granite-greenstone terrane: *Nature*, v. 357, p. 491–493.
- Marshall, B., Giles, A.D., Hagemann, S.G., 2000, Fluid inclusion in metamorphosed and synmetamorphic (including metamorphogenic) base and precious metal deposits: Indicators of ore-forming conditions and/or ore-modifying histories?: *Reviews in Economic Geology*, v. 11, p. 119–148.
- Morey, G.B., 1999, High-grade iron ore deposits of the Mesabi Range, Minnesota—product of a continental-scale Proterozoic ground-water flow system: *ECONOMIC GEOLOGY*, v. 94, p. 133–142.
- Morris, R.C., 1980, Magnetite-hematite relations in the banded iron formations in the Hamersley iron province of Western Australia: *ECONOMIC GEOLOGY*, v. 75, p. 184–209.
- 1983, Supergene alteration of banded iron formations, *in* Trendall, A.F., and Morris, R.C., eds., *Iron formations: Facts and problems*: Amsterdam-New York, Elsevier, p. 513–532.
- Müller, G., Schuster, A.K., and Hoefs, J., 1986, The metamorphic grade of banded iron formations: Oxygen isotope and petrological constraints: *Fortschritte der Mineralogie*, v. 64, p. 163–185.
- Noce, C.M., 1995, Geocronologia dos eventos magmáticos, sedimentares e metamórficos na região do Quadrilátero Ferrífero, Minas Gerais: Unpublished Ph.D. thesis, São Paulo, Brazil, Universidade de São Paulo, 128 p.
- Pires, F.R.M., 1995, Textural and mineralogical variations during metamorphism of the Proterozoic Itabira Iron Formation in the Quadrilátero Ferrífero, Minas Gerais, Brazil: *Anais Academia Brasileira de Ciências*, v. 67, p. 77–105.
- Powell, C.McA., Oliver, N.H.S., Li, Z.-X., Martin, D.McB., and Ronaszecki, J., 1999, Hypogenic hydrothermal origin for giant Hamersley iron oxide ore bodies: *Geology*, v. 27, p. 175–178.
- Ramsay, J.G., 1962, Interference patterns produced by the superposition of folds of similar types: *Journal of Geology*, v. 70, p. 466–481.
- Renger, F.E., Noce, C.M., Romano, A.W., and Machado, N., 1994, Evolução sedimentar do Supergrupo Minas: 500 Ma de registro geológico no Quadrilátero Ferrífero, Minas Gerais, Brasil: *Geonomos*, v. 2, p. 1–11.
- Richards, J.P., and Kerrich, R., 1993, Observations of zoning and fluid inclusions in pyrite using a transmitted infrared light microscope: *ECONOMIC GEOLOGY*, v. 88, p. 716–723.
- Rios, F.J., Fuzikawa, K., Alves, J.V., and Correia Neves, J.M., 2000, O uso da luz infravermelha no estudo petrográfico e de inclusões fluidas em minerais opacos: *Revista Brasileira de Geociências*, v. 30, p. 783–785.
- Roedder, E., 1984, Fluid inclusions: *Reviews in Mineralogy*, v.12, 641 p.
- Romano, A.W., 1989, Évolution tectonique de la région nord-ouest du Quadrilátero Ferrífero—Minas Gerais—Brésil (Géochronologie du socle—Aspects géochimiques et pétrographiques des Supergroupes Rio das Velhas et Minas): Unpublished Ph. D. thesis, University Nancy, 259 p.
- Rosière, C.A., 1981, Strukturelle und Textuelle Untersuchungen in der Eisenerzlagertaette “Pico de Itabira” bei Itabirito, Minas Gerais, Brasilien: *Clausthaler Geowissenschaftliche Dissertationen* 9, 302 p.
- Rosière, C.A., and Chemale, F., Jr., 1991, Textural and structural aspects of iron ores from Iron Quadrangle, Brazil, *in* Pagel, M., and Leroy, J.L., eds., *Source, transport and deposition of metals: Society for Geology Applied to Mineral Deposits Anniversary Meeting, 25th, Nancy, Proceedings*, p. 485–489.
- Rosière, C.A., Chemale, F., Jr., and Guimarães, M.L.V., 1993, Um modelo para a evolução microstrutural dos minérios de ferro do Quadrilátero Ferrífero. Parte I—estruturas e recristalização: *Geonomos*, v. 1, p. 65–84.
- Rosière, C.A., Quade, H., Siemes, H., Chemale, F., Jr., and Resende de Souza, E.M., 1996, Um modelo para a evolução microstrutural dos minérios de ferro do Quadrilátero Ferrífero. Parte II—trama, textura e anisotropia de susceptibilidade magnética: *Geonomos*, v. 4, p. 61–75.
- Rosière, C.A., Chemale, F., Jr., Vanucci, L.C., Guimarães, M.L.V., Carbonari, F.S., Carmo, J.A., Jr., 1997, A estrutura do Sinclínório de Itabira e a tectônica transcorrente do NE do Quadrilátero Ferrífero: *Simpósio Nacional de Estudos Tectônicos (SNET)*, 1997, Pirenópolis, Proceedings, p. 225–226.
- Rosière, C.A., Siemes, H., Quade, H., Brokmeier, H.-G., and Jansen, E.M., 2001, Microstructures, textures and deformation mechanisms in hematite: *Journal of Structural Geology*, v. 23, p. 1429–1440.
- Rosière, C.A., Siemes, H., Rios, F.J., and Quade, H., 2002, Deformation controlled high-grade iron ores [ext. abs.]: *Quadrennial IAGOD Symposium and Geocongress, 11th, Windhoek, Namibia, Geological Survey of Namibia, CD-ROM*.
- Schobbenhaus, C., Campos, D.A., Derze, G.R., and Asmus, H.E., 1984, Mapa geológico do Brasil e da área oceânica adjacente incluindo depósitos minerais, escala 1:2.500.000: Ministério das Minas e Energia, Departamento Nacional da Produção Mineral, Brasília, Brazil.
- Siemes, H., Klingenberg, B., Rybacki, E., Naumann, M. Schäfer, W., Jansen, E., and Rosière, C. A., 2003, Texture, microstructure and strength of hematite ores, experimentally deformed in the temperature range 600° to 1100°C and at strain rates between 10⁻⁴ and 10⁻⁶s⁻¹: *Journal of Structural Geology*, v. 25, p. 1371–1391.
- Schorscher, H.D., 1975, *Entwicklung des polymetamorphen prä-kambrischen Raumes Itabira, Minas Gerais, Brasilien*: Unpublished Ph.D. thesis, University of Heidelberg, 302 p.
- Taylor, D., Dalstra, H.J., Harding, A.E., Broadbent, G.C., and Barley, M.E., 2001, Genesis of high-grade hematite ore bodies of the Hamersley province, Western Australia: *ECONOMIC GEOLOGY*, v. 96, p. 837–873.
- Trendall, A.F., and Blockley, J.G., 1970, The iron formations of the Precambrian Hamersley Group, Western Australia: *Geological Survey of Western Australia Bulletin* 119, 366 p.
- Van Hise, C.R., and Leith, C.K., 1911, The geology of the Lake Superior region: U.S. Geological Survey Monograph 70, 641 p.